SAG: Stars and Galaxies **Vol. 7**, id. 7, 2024 December 28

Study of spectral variability by spectroscopic observation of recurrent nova / symbiotic stars T CrB

Kazuko Ando [1,*], Toshimitsu Toda [1], Shuichi Nakagawa [1], Syoki Muraoka [1], Tomohito Oshima[2], Kenta Taguchi[3,4], and
Naoya Fukuda [1]

[1]*Okayama University of Science, 1–1 Ridaicho, Kita-ku, Okayama-shi 700–0005, Japan*
[2]*Nishi-Harima Astronomical Observatory, Center for Astronomy, University of Hyogo, 407–2 Nishigaichi, Sayo-cho, Hyogo 679–5313, Japan*
[3]*Okayama Observatory, Kyoto University, 3037-5 Honjo, Kamogata-cho, Asakuchi, Okayama 719-0232, Japan*
[4]*Department of Astronomy,KyotoUniversity, Kitashirakawa-Oiwake-cho, Sakyo-ku, Kyoto 606–8502, Japan*
[*]*Kazuko.ando02@gmail.jp*

(Received 2024 October 31; accepted 2024 December 11)

Abstract

T CrB is a recurrent nova that has attracted attention because of several nova explosions in the past. This object is a binary of a white dwarf and a red giant (M3III), and it is also known that semi-regular variability is observed because the apparent size of the photosphere changes due to the orbital motion (P = 227.55 d) of the binary star. This object was reported to have been in active-state from 2015 to 2023, and began to fade from March 2023. Since T CrB showed the temporary dimming just before previous nova eruption, it might be a sign of the nova eruption, but the nature of this phenomenon is still under discussion. We have performed 14 nights low-resolution spectroscopic observations from April 2016 to May 2019, when it was just in the active-state, and 4 nights spectroscopic observations (including 1 night medium-resolution spectroscopic observations) from February 2023 to July 2024, when it was in the temporary-dimming phase. In this paper, we compare our previous observations with the photometric results of the Kamogata Kiso Kyoto Wide-field survey (KWS) and summarize the spectral variations by different phase.

Key words: nova_1 — symbiotic stars_2 — cataclysmic stars_3

1. Introduction

The eruption of T CrB was discovered by J. Birmingham, on 12 May 1866, with his report "very brilliant of about the 2 d mag" (Huggins 1866). In a following report (J. Baxendell), it appears that it was also reported to be at 3.6 or 3.7 magnitude on 15 May (Huggins 1866). Eighty years later, on 9 February 1946, N. F. H. Knight, and then A. J. Deutsch discovered that the object had again brightened, and thus became a recurrent nova (Morgan & Deutsch 1947). Schaefer (2023) focused on the 80 years explosion interval for T CrB, and reported that T CrB may have been erupted in 1217 and 1787 on the past.

Walker (1977) reported that T CrB is a binary star and can be assumed to a symbiotic star model based on its spectral features, including the fact that it shows an infrared excess in late-type stars. T CrB is a binary of a white dwarf and a red giant (M3III) with an orbital period of P = 227.55 d (e.g. Fekel et al. 2000). And red-giant stars are ellipsoidal modulation and are known to exhibit semi-regular variable due to gravitational darkening effects (Zamanov et al. 2004).

It was suggested by Shaefer that it would undergo a nova eruption in 2026, since the 80-year period seen in this object (Schaefer 2010). However, it changed from a low-state to a high-state plateau in 2015, 60 years since the last eruption. Then, in March 2023, the nova eruption began to extinction, which was also seen in the signs of the nova eruption of 1946, and the expected nova eruption date was moved forward and proposed to be 2024.4 ± 0.3[1]. ANS Collaboration[2] observations around late August or early September 2023 reported that the brightness of the accretion disk was minimum and the emission lines temporarily disappeared from the spectrum. It also recovered soon after the minimum, and was observed on 12 January 2024 at U = 11.715, 1.4 times brighter than during the minimum around late August to early September 2023, and the disk was reported to be 6 times more bright than during the minimum when corrected for the contribution of the red giant star (Atel 16404). Two open questions remain about the characteristics of the T CrB light curve, the first of which is the temporary dimming prior to nova eruptions, which was

[1] Schaefer, B. E. 2024, AAS Meeting, 24322505
[2] ANS Collaboration : Asiago Novae and Symbiotic stars collaboration

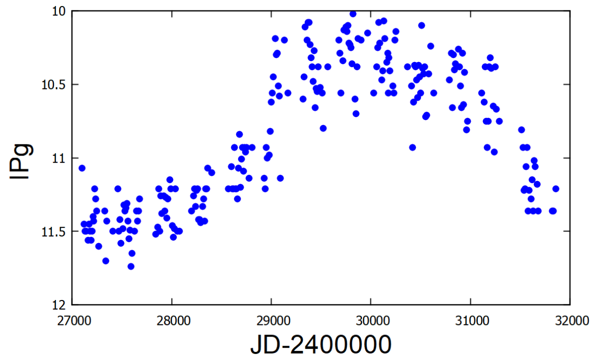

Fig. 1. Light curve of T CrB from 1941/1/15 - 1946/2/3 (plotting from the data of Payne-Gaposchkin and Wright (1946)). The vertical axis is the International Photographic Magnitude (IPg).

noted in the precursor to nova eruptions. Payne-Gaposchkin and Wright (1946) summarized the results of photometric observations with photographic plates before the nova eruption of 1946 (figure 1). Their observations suggest the possibility of several small nova-like eruptions prior to the nova eruption, with the 1946 nova eruption occurring shortly after the light curve, which shows a final brightening a few years before the nova eruption, and a dimming after the last brightening. Observations of Munari et al. (2024) between 2015 and 2023 are similar to precursors to nova eruptions such as those seen in Payne-Gaposchkin and Wright (1946) , suggesting that the timing of the T CrB nova eruption is imminent in Munari et al. (2024).

Spectra showed only small flare events after the nova eruption in 1946, and no photosphere-derived emission lines (e.g. Iijima 1990; Munari et al. 2016). T CrB has been reported super active state once so far. The super active state is characterized by an increase in average brightness (ΔB = 0.72), disappearance of the B-band to ellipsoidal variation, strong He II 4686 emission lines, strong O III and N III associated with the Bowen fluorescence mechanism, and changes in the same phase as He II 4686 (Munari et al. 2016) . This super active state was reported by Hachenberg and Wellmann (1938) on 28 August 1938. The period of super active state at this time was reported to be short, returning to low state on 22 September 1938. A high state was briefly reported by Zamanov and Marti (2001) from 1996 to 1997, but this high state ended by 1998. After the super active state in 1938, it was reported to have entered the super active state in 2015, about 70 years after the nova eruption in 1946, based on the increase in mean brightness (ΔB = 0.72) and intensity of highly excited emission lines. It then reached its maximum in April 2016, and the super active state is thought to have ended in mid-2023. Spectroscopic observations were obtained by Zamanov et al. (2024a) from September 2022 to January 2024, and a double peak was observed in the Hα line during a specific period. Assuming that the double-peaked emission is an accretion disk, the disk radius is $R_{\rm disk}$ = 89 $\pm$ 19 $R_{\odot}$, suggesting that it extends to the Roche lobe of the white dwarf.

Our observations were conducted from April 2016 to May 2019, just during the active-state, and from February 2023 to July 2024, during the temporary-dimming period. In this paper, we summarize the results of these observations.

2. Observation and data analysis

We obtained 18 optical spectra with two telescopes: the Okayama University of Science Observatory (OUSO) 28 cm telescope and the 101 cm telescope at Ibara Bisei Astronomical Observatory (BAO) in Okayama, Japan. The observation at OUSO were performed from 8 April 2016 to 3 May 2019. OUSO telescope is equipped with an SBIG spectroscope DSS-7 and an SBIG CCD camera (ST-402 or ST-1603). The wavelength range covers 3800–7800 Å, with a spectral resolution of R = 400. The data reduction was performed using the BeSpec free software package (developed by Bisei observatory researcher K. Kawabata).

And the observations at BAO were done from 5 February 2023 to 21 July 2024. The telescope is equipped with a spectrograph and a CCD camera (ANDOR DU-440BV). Resolution, the low-medium-resolution spectroscopy is R = 1500, medium-resolution spectroscopy is R = 15000, and the each wavelength range covers 3800–8200 Å, 6400–6800 Å, respectively IRAF was used for data analysis.

3. Results

3.1. *Light curve from 2002 to 2024*

Figure 2 shows photometric observations obtained by the AAVSO[3] from August 2002 to October 2024. The B magnitude began to brighten around May 2014, B = 11.642 $\pm$ 0.097 on 3 May 2014, and reached a maximum (B = 9.93 $\pm$ 0.02) in April 2016, showing a slow decline and then a rapid increase in September 2017 and January 2018. After that, it shows a slow variable. The dates of our observations were marked by the dotted lines in figure 2.

3.2. *Low-resolution spectra at OUSO*

We show the results of low-resolution spectroscopic observations that we have obtained at OUSO. OUSO observation dates up to the five dotted lines from the left in figure 2. Figure 3 shows the observation results offset by an arbitrary value. The emission lines for Hα, Hβ, He I 6678, He I 5876, Fe II + He I 4922 were detected during this period. A prominent emission line was seen in 6029 Å only in the spectrum on 29 April 2016. Iijima (2015) discussed an unidentified line at 6028.3 Å. It suggested that the 6028 Å emission line was probably dependent on highly ionized ions such as [O IV]. However, the reason for the emission line appearance is unclear, as there was no continuous detection of [O IV] 6105.5 Å as seen in Iijima (2015). The EWs of selected emission lines are given in table 1.

3.3. *Low-medium-resolution spectra for BAO*

We show the results of low-medium-resolution spectroscopic observations that we have obtained at BAO. The four dotted lines on the right shown in figure 2 correspond to the observation dates. Figure 4 shows the observation results offset by an arbitrary value. The emission lines for Hα, Hβ,

[3] AAVSO:the American Association of Variable Star Observers

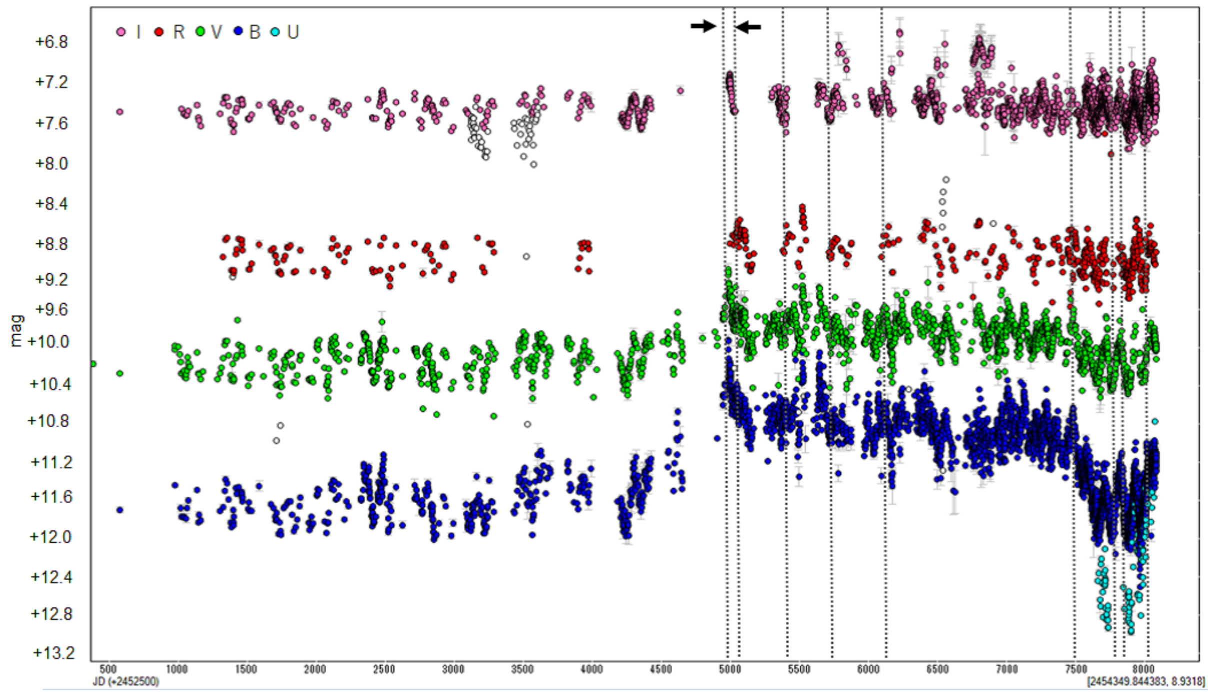

Fig. 2. Light intensity curves using AAVSO data. The two arrows show the 11 nights spectral observation period in 2016, and the three dotted lines across the right side show the spectral observations from 2017 to 2019. The remaining right dotted lines are for the 4 nights spectral observation period 2023–2024.

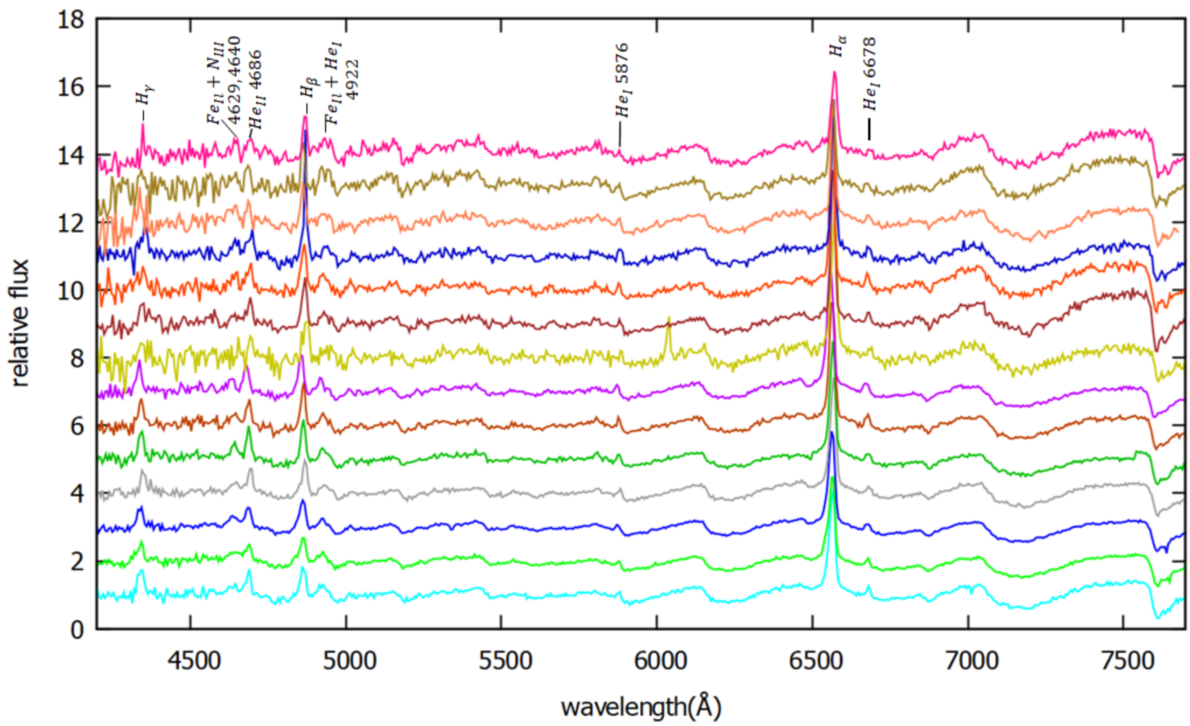

Fig. 3. Low-resolution spectra obtained at OUSO. The time sequence is from the bottom to the top. The spectra are offset by arbitrary values.

Table 1. EWs of selected emission lines. EW was obtained by Gaussian fitting and integrating with wavelength.

Elem	λ[Å]	8 Apr 2016	9 Apr 2016	11 Apr 2016	14 Apr 2016	15 Apr 2016	18 Apr 2016	19 Apr 2016
He II	4686	0.43	0.44	0.46	0.57	0.59	0.61	0.51
Hβ	4861	0.5	0.36	0.53	0.51	0.58	0.6	0.54
He I	5876	0.09	0.01	0.04	0.06	0.07	0.13	0.15
Hα	6562	0.9	0.88	0.89	0.9	0.89	1.23	0.92
He I	6678	0.2	0.05	0.09	0.19	0.2	0.19	0.18

Elem	λ[Å]	29 Apr 2016	11 May 2016	18 May 2016	1 Jun 2016	20 Jul 2017	9 May 2018	3 May 2019
He II	4686	0.60	0.53	0.39	0.42	0.4	0.54	0.32
Hβ	4861	0.77	0.67	0.59	0.88	0.59	0.91	0.71
He I	5876	0.24	0.17	0.14	0.24	0.05	0.05	0.12
Hα	6562	1.2	0.99	1.41	1.24	0.8	0.75	0.92
He I	6678	0.23	0.26	0.38	0.23	0.22	0.12	0.2

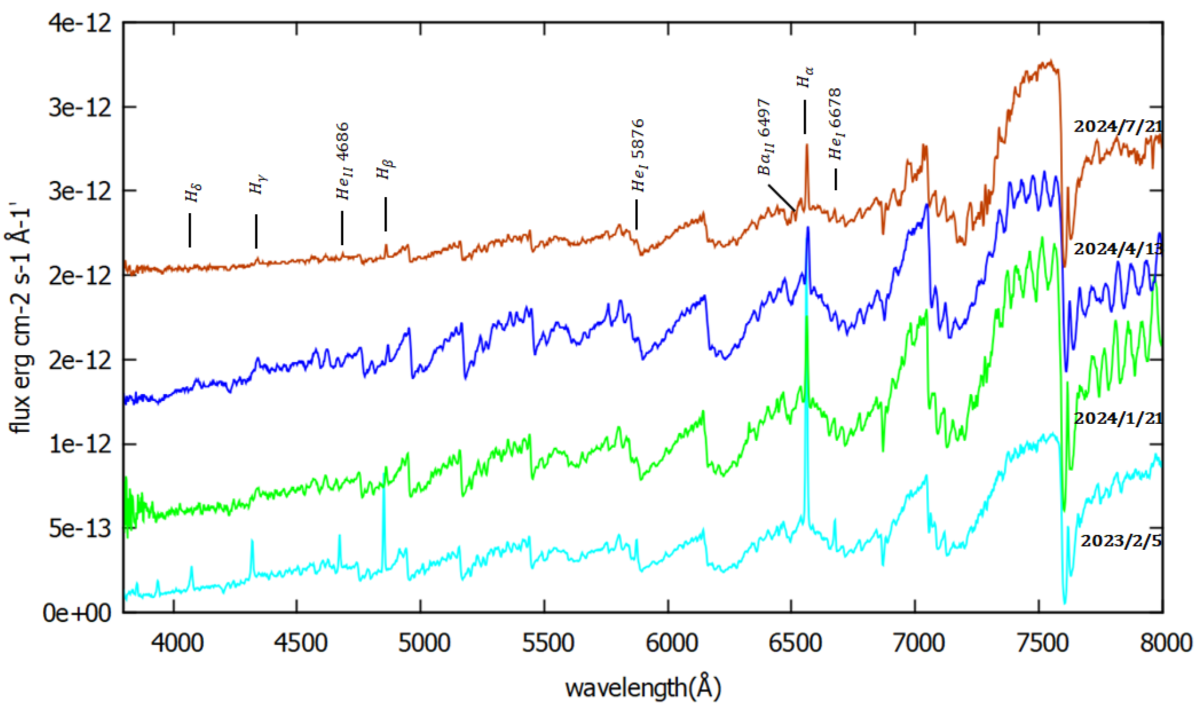

Fig. 4. Low-medium-resolution spectra obtained at BAO.

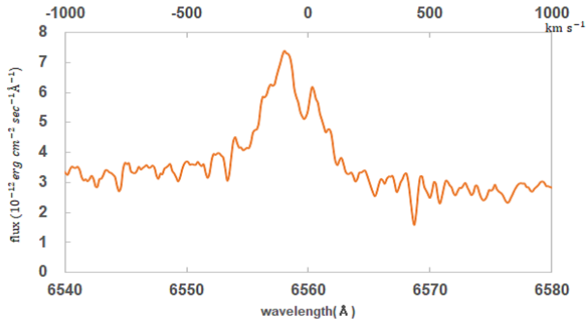

Fig. 5. Spectra around Hα of medium-resolution spectroscopic observations at BAO. The lower horizontal axis is the wavelength, and the upper horizontal axis is the velocity converted from the wavelength. The vertical axis is flux.

He I 6678, He I 5876 and He II 4686 were detected during this period. The resolution at BAO is about 3 times better than that at OUSO. Therefore, Ba II 6497 is more clearly visible in the BAO spectra, although it was also detected with the OUSO observations. Fe II + He I 4922 and Fe II 4629 + N III 4640 seen in 2016 are not seen. The Balmer lines of hydrogen were strongly detected on 5 February 2023, but become weaker after 21 January 2024. This was also true for the other emission lines. He II 4686 was only seen on 5 February 2023 and 21 July 2024. Table 2 lists the prominent emission lines in figure 4.

3.4. *Medium-resolution spectra for BAO*

In this section we show the results of medium-resolution spectroscopic observations, that we have obtained at BAO. The observation on 13 April 2024. The central wavelength is 6560 Å. A double peak was observed at Hα emission line (figure 5), which was not seen in the low-resolution spectroscopic observation.

4. Discussion

In this section, we first discuss the relationship between the intensity change and the phase of the obtained spectra. Figure 6 shows the EWs of the He II 4866, Hβ, Fe II + He I 4922, Hα and He I 6678 emission lines at OUSO in 2016 (table 1) and the light curves for B, V, and Ic magnitude using KWS[4] data (Maehara 2014). The spectral intensities of Hα and Hβ were weak in the early stages of brightening, spring 2016. There was also a trend toward stronger Hα intensity and weaker He II 4686 in the sense of about 23 days from 29 April 2016. Figure 7 shows the same as figure 6 but for the period from 2017 to 2019. Only the Fe II + He I 4922 emission lines showed a trend of strengthening, while no significant changes were observed for the other emission lines.

Iijima (1990) discussed the 1981–1990 high and low states of this object and suggested that the decrease of emission line intensity is the result of a decrease of mass transfer rate, not eclipse. Peel (1985) proposed a binary star model with elliptical orbits, which suggested that the mass transfer rate varies periodically. Iijima (1990) suggested that the pulsation period of M-type giant stars may be involved. However, Belczynski and Mikołajewska (1997) argue that the 55-day period is not due to pulsation, since the light curve and color characteristics behave like opposite way seen in pulsating M giants. Munari et al. (2016) also reported that when the object is in the low state, the ellipsoid variation of red-giant stars is clearly visible in the $BVRI$.

To study the relationship between our spectra and the phase, we determined the period using periodic analysis (PDM method[5]) for the AAVSO's B-band light curve from 1 January 2000 to 31 December 2012, which is considered to be a quiescent period. We obtained two kind of period. The shorter one is P = 113.658579(5) d and the long one is P = 227.5687(5) d. The long one is the orbital period and the short one is half of the period. T CrB has an eccentricity of $e = 0.008 \pm 0.012$ (Fekel et al. 2000) , and since it has a nearly circular orbit, it is expected to produce a period of half the orbital period naturally. From the period obtained here, we defined MinB = 2455600.69 as the epoch of primary minima. This date of MinB is not contradictory with MinI = 2431933.83 + 227.55 $\times$ E in Munari et al. (2016) for E = 104. When we performed the same periodic analysis extended to 22 October 2024. We obtained longer period of P = 277.830257(5) d, which was 50.261557(3) d longer than the previous period of 227.5687 d. It is possible that short periods overlap after the 2015 active state. Iłkiewicz et al. (2016) found that the short one was P = 87 d in VRI, and the long one was P = 114 d in V. Our analysis also detected P = 89.121734(5) d. Epoch at this phase was aligned with Munari et al. (2016). The periodic analysis for the post 2014 pre-active state period shows no periodicity, although PDM minima can be detected as described above (figure 8). Therefore, a simplified diagram of the phase during the OUSO and BAO observations is shown in figure 9 for the results of the periodic analysis for P = 227.5687 d obtained from the light curve for the quiescent period. The figure here does not take into account the binary parameters (mass, binary distance, and inclination). Figure 10 summarizes the fluxes of the emission lines of BAO. The intensity of Hα decreased significantly, especially from 2023 to 2024. Other emission lines are also decreasing, although not as much as Hα. These results suggest that there is no significant correlation between phase and spectral intensity changes.

Given the non-conclusive relationship between spectrum and orbital phase, we consider factors that would cause the spectrum to vary outside of phase, such as pulsation activity, for example, as suggested by Iijima (1990). Figure 11 shows the results of the periodic analysis of the AAVSO light curves (B, V, I) from 7 February 2011 to 31 December 2012, a quiescent season. The orbital phase folded from primary minima to P = 277.5687 d. Here, the images are superimposed to make it easier to see the phase differences observed in the periodic analysis. The light curves of I and V bands are found to correlate with the location of the conjunctions of the red giants. The B band behaves similarly to the V band, but shows variation due to the complex mixing of multiple periods. Activity due to pulsation could not be considered from this period.

4 KWS : Kamogata Kiso Kyoto Wide Field Survey (Maehara 2014)

5 This research used Peranso (www.peranso.com), a light curve and period analysis software (Paunzen & Vanmunster 2016).

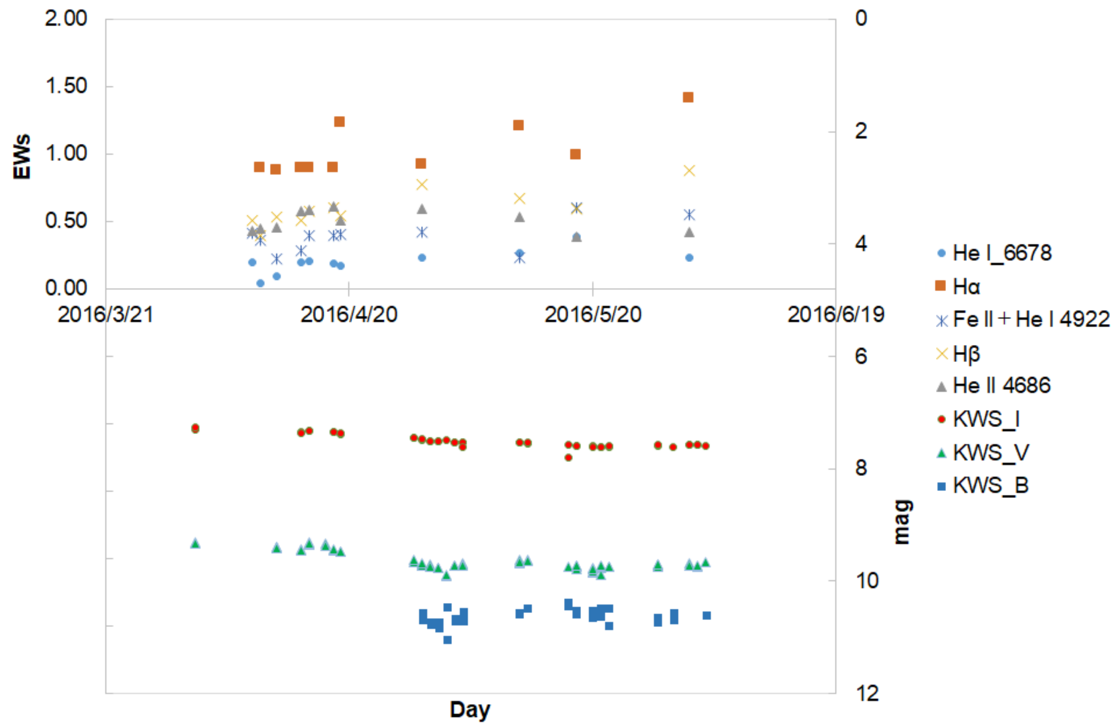

Fig. 6. Time evolution for EWs at OUSO (2016). In the upper panel, He II 4866, Hβ, Fe II + He I 4922, Hα and He I 6678 emission lines. The upper panel shows the EWs. The horizontal axis is date, and the left axis is EW. The lower panel shows the light curve of KWS. The horizontal axis is date, and the right axis is mag.

Fig. 7. Time evolution for EWs at OUSO (2017–2019). In the upper panel, He II 4866, Hβ, Fe II + He I 4922, Hα and He I 6678 emission lines. The upper panel shows the EWs. The horizontal axis is date, and the left axis is EW. The lower panel shows the light curve of KWS. The horizontal axis is date, and the right axis is mag.

Table 2. Intensities of selected emission lines. The flux values at the emission line peak.

		Flux			
Elem	λ[Å]	2023/2/5	2024/1/21	2024/4/13	2024/7/21
Hγ	4340	4.25	2.36	3.11	0.95
He II	4686	4.63	-	-	1.25
Hβ	4861	8.28	3.62	3.89	1.812
He I	5876	4.30	4.08	4.27	2.09
Hα	6562	22.16	12.58	10.92	7.83
He I	6678	5.46	6.51	5.83	3.90

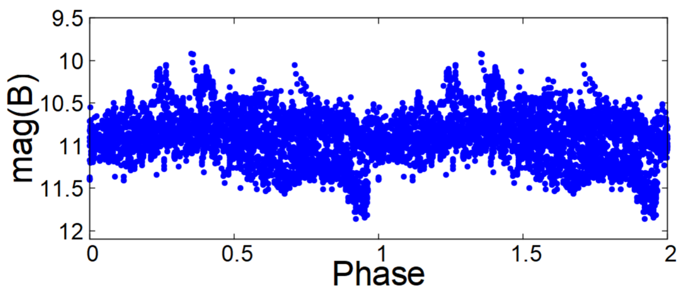

Fig. 8. Phase-folded light curves from the AAVSO light curves. Light curve from 2016/1/1 to 2023/7/1 folded at 227.5687 d, considered to be during super active state.

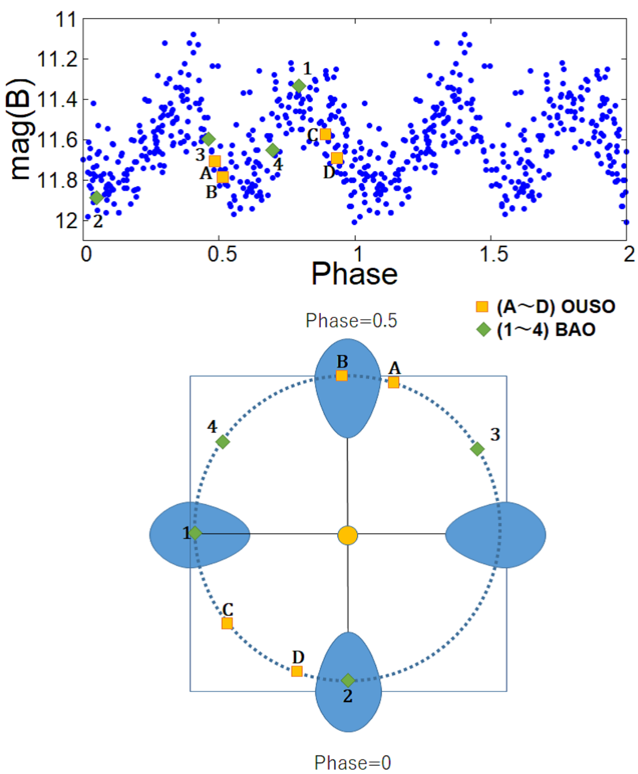

Fig. 9. Phase diagram of the OUSO and BAO observations. The upper panel is the phase folded at P = 227.5687d. The lower panel is an imaginary diagram of the phase. Labels A–D on the lower panel are the phases for the observation dates, see appendices. Labels 1–4 on the lower panel are the phases for the observation dates, see appendices.

Finally we discussed three states of T CrB. T CrB has been reported to show three states: low, high (Iijima 1990) and super active states (Munari et al. 2016). In high state, both the emission lines and nebular continuum are strong, and the emission lines change within 55 days. The super active states were characterized by the presence of O IV and [N V] lines, very strong He II 4686 and a strong blend of 4640 Bowen fluorescence, a large increase in mean brightness, and the disappearance of orbital modulation from the B band light curve. The most recent super active state occurred in 2015–2016 and reached its maximum in April 2016 (e.g. Munari et al. 2016; Zamanov et al. 2024b). For the past super active states, the transition to the low state took less than one month, slightly different from the current super active state. Our observations would cover this high to low state. During this period (2016/8/4–2019/3/5) OUSO spectra showed strong He II 4686 and strong 4640 Bowen fluorescence blends and strong Balmer lines, which would be characteristic of a super active state. Figure 12 shows the BAO spectrum around the He II 4686 and Hβ spectra offset by arbitrary values. The He II 4686 emission line was clearly visible on 5 February 2023 but disappeared both on 25 January and on 13 April 2024. It suggested that the state of T CrB changed from super active to low. The He II 4686 emission line appeared again on 21 July 2024, but was weaker than that on 5 February 2023. Munari et al. (2016) summarizes that the emission lines in the spectra after the 1946 outburst were mainly Balmer and H I lines, no He II 4686 emission

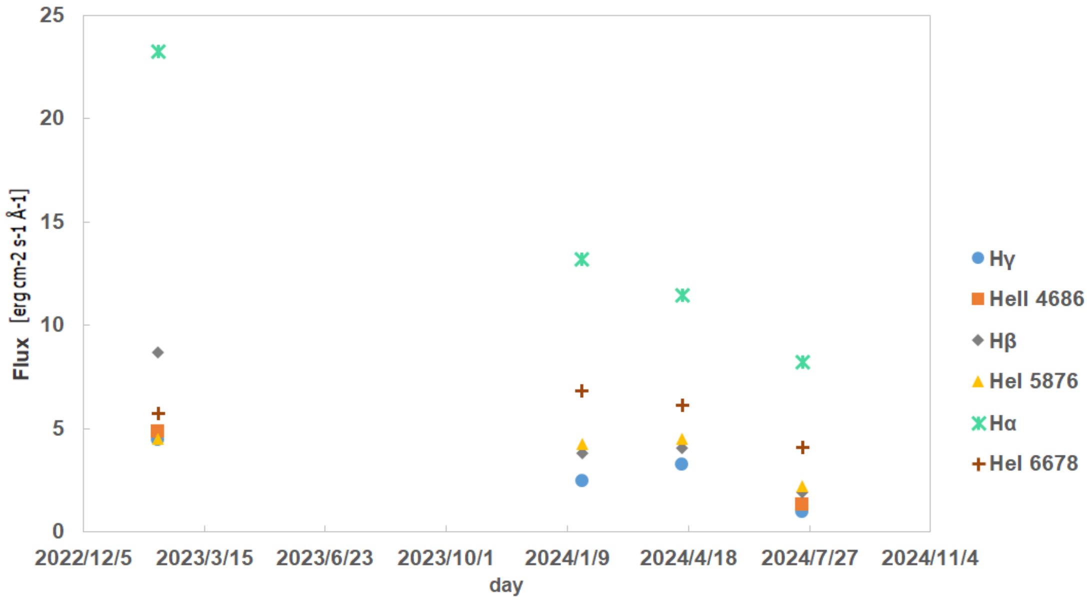

Fig. 10. Flux of the emission lines of BAO (2017-2019). The horizontal axis is Day, and the vertical axis is Flux.

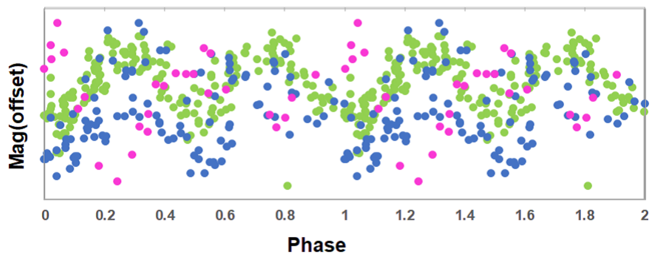

Fig. 11. Phase-folded light curves from the AAVSO light curves (B, V, I). The period was the quiescent period from 7 February 2011 to 31 December 2012.

line were seen (Blair et al. 1983; Williams 1983; Gravina 1981; Kenyon & Garcia 1986; Zamanov and Marti 2001; Munari & Zwitter 2002). Only Iijima (1990) reported a weak Balmer and He II 4686 emission line during 1982–1987. The He II 4686 emission line seen on 21 July 2024 would be similar to the one he reported.

Hα emission line profiles would also change as to the state. In the low state, a double peak was seen in Hα on 23 April 2013 (Munari et al. 2016). The super active state, Hα on 23 October 2015, has a single peak. Furthermore, Zamanov et al. (2024a) reports a double peak between July 2023 and January 2024. The Hα emission lines were weakest between August and October 2023, which may indicate a transition to the low state at this time. The Hα emission in the super active state is thought to come from the ionized winds of red-giant stars (Munari 2023). The double peak of Hα seems to be an indication of the transitional period between super active sate and low state. The double peak of the Hα line observed from the end of the super active state was assumed to be radiation from

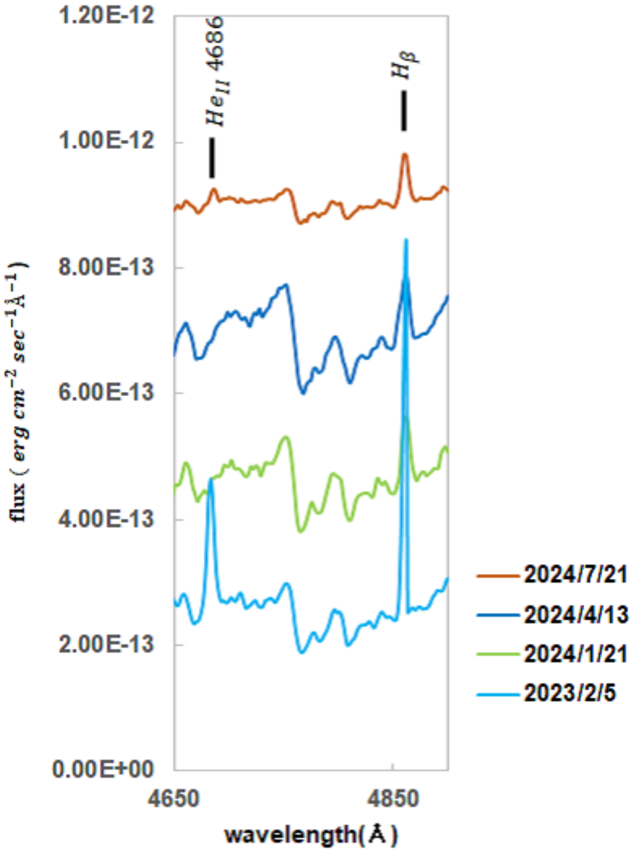

Fig. 12. Spectra of He II 4686 and Hβ observed at BAO. The horizontal axis is a wavelength, in the wavelength range 4650–4855 Å. The vertical axis is flux, offset by an arbitrary value.

the accretion disk around the white dwarf, and Zamanov et al. (2024a) estimated the mean radius of the accretion disk. Our 13 April 2024 low-medium-resolution spectroscopic observations also showed a double peak in Hα, so we estimated the radius of the disk in the same way (figure 5). Assuming that the double peak is emitted from the Kepler disk, Δv = 113.27 km s^{-1} and the disk size is $R_{\rm disk}$ = $70R_{\odot}$. This value is within the disk radius range evaluated by Zamanov et al. (2024a). Then the Roche lobe (mean $R_{\rm disk}$ = 89 $\pm$ $19R_{\odot}$) is found to be in an unfulfilled state.

Mass transfer from a red giant star distorted by the tidal forces filling the Roche lobe results in a disk similar to that of a cataclysmic variable star. Symbiotic stars can be divided into symbiotic novae and classical symbiotic novae based on their activity (Mikołajewska 2011). Symbiotic novae are thermonuclear novae in symbiotic binary stars. Classical symbiotic novae are caused by thermal pulses or shell flashes (Kenyon & Truran 1983) and disk instabilities for dwarf nova (Munari & Zwitter 2002). We supposed that the 2016 outburst was a classical symbiotic nova triggered by disk instability, and the expanding shell formed. Shell ejections have also reported in classical symbiotic outburst. T CrB was suggested to be closely related to SU UMa-type dwarf novae with very long orbital periods (Iłkiewicz et al. 2023). This active state may also be due to disk instability. We believe that continued observations will lead to the solution of the mystery of the pre-eruption dimming and the secondary maximum.

Acknowledgments

The authors are indebted to all the staff of BAO for their continuous support during the observations. We acknowledge with thanks the variable star observations from the AAVSO International Database contributed by observers worldwide and used this research. We also thank the referee for improving the manuscript.

Appendix 1. Table 3: OUSO

Appendix 2. Table 4: BAO

Appendix 3. Table 5: Observation log

References

Belczynski, K., & Mikołajewska, J. 1997, MNRAS, 296, 77
Blair, W. P., Stencel, R. E., Feibelman, W. A., & Michalitisianos, A. G. 1983, ApJS, 53, 573
Fekel, F. C., Joyce, R. R., Hinkle, K. H., & Skrutskie M. F. 2000, AJ, 119, 1375
Gravina, R. 1981, IBVS, 2041, 1
Hachenberg, O., & Wellmann, P. 1938, Astronomische Nachrichten, 266, 375
Huggins, W. 1866, MNRAS, 26, 275
Iijima, T. 1990, JAVSO, 19, 28
Iijima, T. 2015, AJ, 150, 20
Iłkiewicz, K., Mikołajewska, J., Stoyanov, K., Manousakis, A., & Miszalski, B. 2016, MNRAS, 462, 2695
Iłkiewicz, K., Mikołajewska, J., & Stoyanov, K. A. 2023, ApJL, 953, 7
Kenyon, S. J., & Truran, J. W. 1983, ApJ, 273, 280
Kenyon, S. J., & Garcia, M. R. 1986, AJ, 91, 125
Maehara, H. 2014, JAXA-RR-13-010, 119
Mikołajewska, J. 2011, arXiv:1011.5657v2
Morgan, W. W., & Deutsch, A. J. 1947, ApJ, 106, 362
Munari, U., & Zwitter, T. 2002, A&A, 383, 188
Munari, U., Dallaporta, S., & Cherini, G. 2016, NewA, 47, 7
Munari, U. 2023, RNAAS, 7, 145
Munari, U., Ochner, P., Dallaporta, S., Valisa, P., Vagnozzi, A., Moretti, S., Bergamini, A., & Cherini, G. 2024, The Astronomer's Telegram, 16404, 1
Paunzen, E. & Vanmunster, T. 2016, Astronomische Nachrichten, 337, 239
Payne-Gaposchkin, C., & Wright, F. W. 1946, ApJ, 104, 75
Peel, M. 1985, JAVSO, 14, 8
Schaefer, B. E. 2010, ApJS, 187, 275
Schaefer, B. E. 2023, Journal for the History of Astronomy, 54, 436
Walker, A. R. 1977, MNRAS, 179, 587
Williams, G. 1983, ApJS, 53, 523
Zamanov, R., & Marti, J. 2001, IBVS, 5013, 1
Zamanov, R., Bode, M. F., Stanishev, V., & Martí, J. 2004, MNRAS, 350, 1477
Zamanov, R. K., et al. 2024a, Astronomische Nachrichten, 345, e20240036
Zamanov, R. K., et al. 2024b, arXiv:2308.04104v2

Table 3. Relation between phase and observation at OUSO. The relationship between the phase of the observation at OUSO (folded at 227.5678 d) and table 3. Lables refer to the labels on the image in figure 10.

Day	Phase	Label
2016/4/8	0.79	C
2016/4/9	0.79	C
2016/4/11	0.80	C
2016/4/14	0.81	C
2016/4/15	0.82	C
2016/4/18	0.82	C
2016/4/19	0.83	C
2016/4/29	0.86	C
2016/5/11	0.91	D
2016/5/18	0.93	D
2016/6/1	0.98	D
2017/7/20	0.46	A
2018/5/8	0.53	B
2019/5/3	0.81	C

Table 4. Relation between phase and observation at BAO. The relationship between observation and phase at BAO is shown in table 4. Labels refer to the labels on the image in figure 10.

Day	Phase	Label
2023/2/5	0.76	1
2024/1/21	0.02	2
2024/4/13	0.32	3
2024/7/21	0.68	4

Table 5. Observation log.

Date	UT	Observatory	R	Wavelength range [Å]
2016/4/8	13:42:49	OUSO	400	3800–7800
2016/4/9	14:31:43	OUSO	400	3800–7800
2016/4/11	14:08:18	OUSO	400	3800–7800
2016/4/14	16:01:10	OUSO	400	3800–7800
2016/4/15	13:26:16	OUSO	400	3800–7800
2016/4/18	14:20:33	OUSO	400	3800–7800
2016/4/19	14:08:34	OUSO	400	3800–7800
2016/4/29	13:42:46	OUSO	400	3800–7800
2016/5/11	11:40:56	OUSO	400	3800–7800
2016/5/18	14:30:34	OUSO	400	3800–7800
2016/6/1	13:09:39	OUSO	400	3800–7800
2017/7/20	11:36:24	OUSO	400	3800–7800
2018/5/9	14:17:57	OUSO	400	3800–7800
2019/5/3	14:08:32	OUSO	400	3800–7800
2023/2/5	17:04:32	BAO	1500	3800–8200
2024/1/21	18:20:25	BAO	1500	3800–8200
2024/4/13	19:24:44	BAO	1500	3800–8200
2024/4/13	16:10:51	BAO	3100	6400–6800
2024/7/21	16:36:50	BAO	1500	3800–8200